Nanoscale Observation of a Grain Boundary Related Growth Mode in Thin Film Reactions

M. Seibt, S. Buschbaum, U. Gnauert,* and W. Schröter
IV.Physikalisches Institut der Universität Göttingen and Sonderforschungsbereich 345, Bunsenstr.13-15, D-37073 Göttingen, Germany

D. Oelgeschläger†
Institut für Metallphysik der Universität Göttingen and Sonderforschungsbereich 345, Hospitalstr.3-5, D-37073 Göttingen, Germany
(Received 29 October 1996)

We report the atomic scale observation of a thin film growth mode related to grain boundaries in multilayers of polycrystalline gold and amorphous silicon. Using differential scanning calorimetry, *in situ* x-ray diffraction, and high-resolution electron microscopy, we observe silicide nucleation to take place at grain boundaries in the polycrystalline gold films followed by lateral silicide growth parallel to gold/silicon interfaces. This growth mode is related to solid-state reactions at low temperatures where atomic transport is restricted to grain and interphase boundaries. It demonstrates the importance of thin film microstructure for phase selection during thin film reactions at low temperatures. [S0031-9007(97)05118-1]

PACS numbers: 81.10.Aj, 61.72.Mm, 81.15.Tv

Metal silicides are of still growing interest as low resistivity contact materials for silicon devices. As device dimensions shrink, the controlled and reliable fabrication of silicides increasingly requires the understanding of basic mechanisms of thin film reactions. Thin film diffusion couples represent nonequilibrium systems frequently exhibiting large driving forces ($\gg k_B T$, k_B: Boltzmann's constant) for phase formation. The final state to which such systems develop is simply determined by the minimum of the Gibbs free energy of the alloy system. The number of intermediate phases accessible by the system increases with increasing driving force. Which of these phases is selected in the early stages of the reaction is determined by the kinetics of the system when it follows the path towards this phase. Frequently, relaxation occurs via metastable intermediate phases, a prominent example being the well-known solid-state amorphization reactions between early and late transition metals [1].

For the high-temperature regime where bulk interdiffusion is possible, bulk thermodynamics and kinetics can be used to describe phase selection in terms of nucleation [2] and growth kinetics [2–5] of the competing phases. It is commonly assumed that the product phase nucleates homogeneously at the interface between the parent phases ("α/β interface") [2] or heterogeneously at triple points with grain boundaries followed by coalescence of the nuclei along the α/β interface [2,6,7]. In both cases, nucleation evolves into the frequently observed planar growth of the product phase.

In the low-temperature regime of negligible bulk diffusion, atomic transport is restricted to defective regions like interfaces, dislocations, and grain boundaries [8–11]. As a consequence, certain intermediate phases may no longer be accessible from the initial state by thermal fluctuations implying bulk thermodynamics and kinetics to be of limited use for the prediction of the reaction path towards equilibrium. Instead, it seems obvious that microscopic details of the available diffusion paths are of increasing importance. This has been recognized in a recently proposed model which uses irreversible thermodynamics to calculate the effective driving force for product phase nucleation in the two-dimensional systems of interphase and grain boundaries [12].

In this Letter, we report the first direct observation at the atomic scale of a thin film growth mode governed by grain boundaries under conditions where homogeneous phase nucleation and bulk interdiffusion are negligible (Harrison's type *C* kinetics [13]). We observe the formation of metastable Au_3Si in multilayers consisting of polycrystalline Au (*c*-Au) and amorphous Si (*a*-Si) to take place at grain boundaries of the *c*-Au films. In contrast to the usually observed planar film growth, x-ray diffraction (XRD) and high-resolution transmission electron microscopy (HRTEM) consistently show *lateral growth* of Au_3Si into the *c*-Au grains, i.e., parallel to *c*-Au/*a*-Si interfaces. HRTEM further reveals epitaxial relations between the formed silicide and adjacent Au grains. This suggests that the formation of low-energy interfaces is an important criterion selecting the silicide *and* the grain boundaries where the phase forms.

Multilayers consisting of *c*-Au and *a*-Si were prepared by evaporation in ultrahigh vacuum at a background pressure of 10^{-9} mbar on (001) Si substrates cooled by liquid nitrogen. Film thicknesses have been varied in the ranges of 2.2–7.8 and 4–20 nm for *c*-Au and *a*-Si, respectively. Differential scanning calorimetry (DSC) measurements were carried out in a Perkin Elmer DSC 7. *In situ* XRD data were obtained in the $\theta - 2\theta$ geometry.

Below the eutectic temperature of 363 °C crystalline Au and Si coexist in thermodynamic equilibrium with

 0031-9007/98/80(4)/774(4)$15.00

small mutual solubilities [14]. However, metastable silicides have been produced by solid state reactions after Au implantation into silicon [15], in Au-Si multilayers [16], and due to Au precipitation in c-Si [17] as well as by rapid quenching from the melt [18,19]. For c-Au/a-Si multilayers the direct path into equilibrium is the crystallization of the a-Si. Instead, three distinct exothermic reactions are obtained corresponding to DSC peaks A, B, and C in Fig. 1. Detailed investigations to identify these reactions using XRD, transmission electron microscopy, and Rutherford backscattering are described elsewhere [20]. Although we shall focus here on the mechanism of metastable Au_3Si formation, a brief description of all reactions is given for completion: DSC peak A at about 100 °C for a heating rate of 10 K/min corresponds to the formation of a metastable gold silicide of composition Au_3Si, followed by metal-induced crystallization of the remaining a-Si (DSC peak B) at about 180 °C. This process has been observed for a number of systems including a-Si:Au [16], a-Si:Ni [21], or a-Ge:Ag [22]. The final reaction (DSC peak C) is the decomposition of the metastable Au_3Si into c-Au and c-Si which coexist in equilibrium below the eutectic temperature.

We first describe *in situ* XRD measurements of the kinetics of silicide formation. In order to monitor the volume fraction and the thickness of the unreacted c-Au layers we have extracted the integrated intensity I_{int} and the width w of the Au{111} diffraction peak, respectively, from *in situ* XRD spectra [23]. Neglecting contributions from strain and interfacial roughness, w is directly related to the thickness d_{Au} of the c-Au films according to Scherrer's law, i.e., $d_{\text{Au}} = 0.9\lambda w^{-1}(\cos\theta)^{-1}$ [24], and I_{int} is related to the volume fraction of unreacted c-Au if the texture is unchanged.

Figure 2 shows the relative intensity $I_{\text{int}}/I_{\text{int}}^0$ (squares) and width w/w_0 (circles) as a function of time for a reaction at 80 °C [25]. The width w of the Au{111} peak initially decreases due to strain relaxation in the layers which is corroborated by the simultaneous shift of the peak position by 0.3% to the value corresponding to the Au lattice parameter at 80 °C. Subsequently, the peak width remains unchanged, indicating *constant* thickness d_{Au} of the remaining Au layers during the reaction. This observation clearly shows that silicide formation proceeds by *lateral* growth along c-Au/a-Si interfaces rather than by growth of planar layers at the interfaces between c-Au and a-Si. Hence, there is evidence of grain boundaries in the c-Au to play an important role in silicide nucleation and growth. Lateral growth contributing to the formation of amorphous nickel silicide in c-Ni/a-Si multilayers has been reported previously [27]. The authors conclude a-NiSi formation also at grain boundaries in the c-Ni from a significantly faster decrease of the integrated intensity I_{int} compared to the peak width w. In our case (Fig. 2) I_{int} is determined by two simultaneous effects, i.e., Au_3Si formation and a change of the c-Au texture as could be verified by electron diffraction. The latter is responsible for the initial increase of I_{int}. Hence, the kinetics of silicide growth cannot be extracted from these data.

In order to gain microscopic information of silicide growth HRTEM investigations were carried out on structures consisting of a single 5.6 nm thick c-Au layer between two 4.5 nm thick a-Si layers. For a direct comparison of DSC and HRTEM data samples were heated *ex situ* at a constant rate (10 K/min) to temperatures between 80 and 120 °C and subsequently quenched to room temperature. A mixture of $HF:HNO_3$ was used to prepare TEM foils in plan view [28]. High-resolution images were obtained at 200 kV using a Philips CM200-FEG-UT. The microscope has a point resolution of 0.188 nm and an information limit of 0.11 nm allowing lattice imaging of c-Au along six different zone axes which is sufficient to detect silicide nucleation in the grain boundaries of the polycrystalline gold films.

As-grown multilayers revealed a growth-induced texture with Au{111} parallel to the growth direction. The grains have a columnar structure with an average grain size of about 40 nm. Heating to 80 °C destroys this

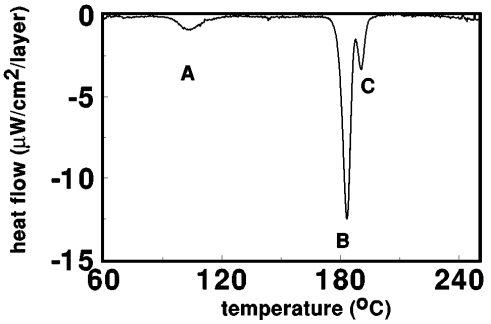

FIG. 1. DSC trace obtained with a heating rate of 10 K/min from a multilayer sample consisting of c-Au and a-Si layers with thicknesses of 5.6 nm and 10.3 nm, respectively. Three distinct exothermic reactions are revealed: (A) silicide formation, (B) metal-induced crystallization of a-Si, and (C) silicide decomposition into c-Au and c-Si.

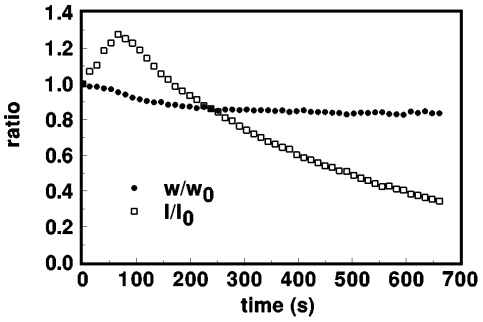

FIG. 2. Relative width w/w_0 (solid circles) and integrated intensity $I_{\text{int}}/I_{\text{int}}^0$ (open squares) of the Au(111) diffraction peak as a function of annealing time obtained at 80 °C; note that after an initial transient the linewidth essentially stays constant indicating constant, thickness of c-Au films during silicide formation.

texture and leads to the formation of a high density of twin boundaries within the grains. At this stage "clean" grain boundaries in the *c*-Au without any evidence for phase formation are obtained [29]. This observation is in agreement with DSC measurements (compare Fig. 1).

Silicide formation was observed in samples heated to temperatures above 95 °C. Fig. 3(a) is a HRTEM micrograph obtained from a sample heated to 95 °C and subsequently quenched. Four different grains are immediately recognized [labeled "1", "2", "3", and "S" in Fig. 3(a)]. Phase identification from lattice images is straightforward in the *a*-Si/*c*-Au system by Fourier transforms of specified areas as illustrated in Fig. 3(b): grains 1, 2, and 3 consist of crystalline Au imaged along ⟨211⟩ (the orientation of grain 2 is slightly off Au ⟨211⟩). The region labeled "S" is a lattice image of the metastable Au_3Si. Lattice spacings of 0.308, 0.295, 0.236, and 0.145 nm are obtained from Fig. 3(e) which agrees with x-ray diffraction data ([16,20]). The majority of experimentally observed silicide grains share lattice planes with at least one of the adjacent (unreacted) Au grains. For the example shown in Fig. 3(a), the silicide has an orientational relationship to grains 1 and 2. The diffractograms of grain 1 and the silicide coincide at point *A* [Fig. 3(f)] which corresponds to an interplanar spacing of 0.144 nm [Au(220)]. Grain 2 and the silicide share diffraction spot *B* [0.236 nm corresponding to Au(111)] showing the silicide to crystallographically mediate between the two Au grains.

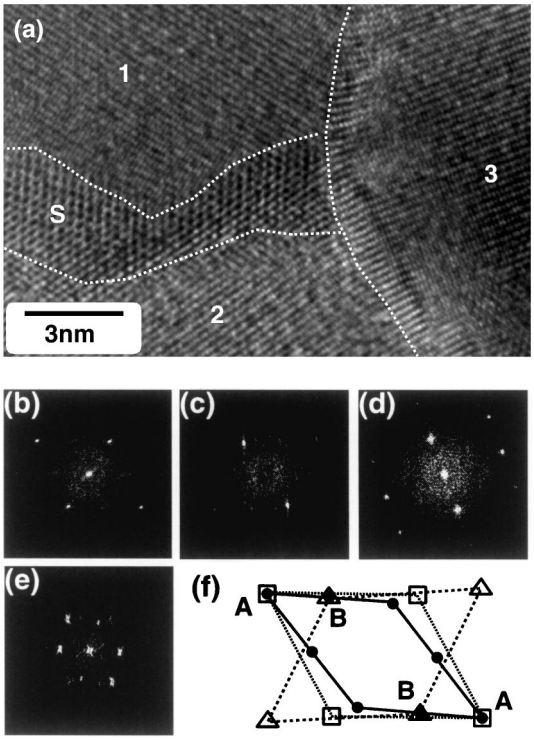

FIG. 3. Silicide nucleation at grain boundaries of the *c*-Au as obtained by high-resolution electron microscopy in plan view; (a) Au_3Si crystallite (labeled "S") and three adjacent Au grains (labeled "1", "2", "3"); phase identification is done by numerically calculated diffractograms shown in (b)–(e): (b) *c*-Au imaged along ⟨211⟩ (grain 1), (c) *c*-Au image along ⟨211⟩ with a slight mistilt (grain 2), (d) *c*-Au imaged along ⟨211⟩ (grain 3), (e) Au_3Si and (f) schematic diffractograms of regions 1 (dotted line and open squares), 2 (dashed line and open triangles), and *S* (solid line and solid circles) showing common reflections of grains 1 and 2 with the silicide, labeled "A" and "B," respectively.

HRTEM images obtained during later stages of phase formation show Au_3Si and *c*-Au grains existing side by side. Hence, *in situ* x-ray diffraction and HRTEM consistently show lateral silicide growth. Furthermore, silicide grains appear to extend through the whole *c*-Au layer during all stages of phase formation which can be concluded from the lack of Moiré fringes which are expected from overlapping crystals along the electron beam direction. This observation strongly suggests silicide nucleation to occur in the grain boundaries rather than heterogeneously at triple points of *c*-Au/*a*-Si interfaces and grain boundaries.

In order to discuss our experimental observations, we have to consider thermodynamic and kinetic properties of the *c*-Au/*a*-Si system. From DSC the driving force for Au_3Si formation has been measured as 1.6 kJ/g atom [20]. Choosing a small interfacial energy of 0.1 J/m^2, a nucleation barrier of 4.6 eV is estimated showing homogeneous nucleation to be virtually impossible at the reaction temperature of about 100 °C. Hence, high energy faults are needed to considerably lower the nucleation barrier in agreement with experimental observations. In fact, Au_3Si formation was not observed at low angle grain boundaries or at $\Sigma 3(111)$ twin boundaries in spite of their high density as a result of recrystallization indicating high-energy large angle grain boundaries to be predominant nucleation sites in this system. At the reaction temperature of about 100 °C, bulk diffusion of Si in *c*-Au and Au in *a*-Si are negligible [30], whereas Si diffusion along grain boundaries in *c*-Au or metastable Au silicides has been concluded from SiO_2 formation on top of *c*-Au above 80 °C [31]. In addition, our observation of recrystallization in the *c*-Au layers preceding silicide formation provides evidence that Au atoms are mobile in *c*-Au grain boundaries, showing that the latter are indeed the dominant if not the only diffusion path in the system, i.e., the system obeys type *C* kinetics [13] in the unreacted state. Our observation of lateral growth is consistent with the assumption that type *C* kinetics also apply for the partially reacted state. Unlike planar growth which is ultimately limited by bulk diffusion through the silicide, lateral growth fed by atomic transport along *c*-Au/Au_3Si interfaces may be possible throughout the reaction. Figure 4 summarizes the thin film growth mode observed under such conditions. Phase nucleation occurs in grain boundaries [Fig. 4(a)] of the *c*-Au, followed by lateral growth from the grain boundaries into the *c*-Au [Fig. 4(b)].

We now consider more general implications of our results. As has been outlined above, *c*-Au and *a*-Si

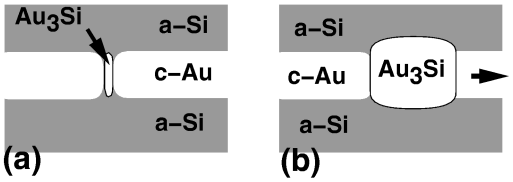

FIG. 4. Schematic representation of the observed mode of thin film reaction: (a) Au_3Si nucleation at grain boundaries of the c-Au followed by (b) lateral growth of Au_3Si parallel to c-Au/a-Si interfaces. Here, we have taken into account that Au_3Si formation proceeds at constant volume as concluded from small angle x-ray diffraction data which show a constant thickness of double layers (a-Si/c-Au or a-Si/Au_3Si) throughout the reaction.

exclusively communicate via grain boundaries which are the only sites allowing silicide nucleation and atomic transport. In these respects the situation is analogous to that during alloy growth from the gas phase. There, phase formation is governed by surface kinetics and thermodynamics since transport is usually restricted to the top atomic layers. Such conditions may lead to metastable phase formation like the long-range ordering during MBE of SiGe [32,33]. Similarly, early stages of phase reaction under conditions of type C kinetics are adequately described in terms of thermodynamics and kinetics of grain boundary "phases". From our experiments we may conclude that the ability of a certain product phase to structurally mediate between adjacent grains is one of the keys to phase selection in grain boundaries. This view is corroborated by the fact that in multilayers containing thick (>21 nm) Au films a different silicide structure is observed by XRD [20] indicating alternative relaxation paths for thick Au films. Hence, there is evidence that microstructural properties of thin films considerably contribute to phase selection in the low-temperature regime.

We gratefully acknowledge stimulating discussions with R. Bormann, H.-U. Krebs, and B. Plikat. Part of this work was financially supported by the Volkswagen-Stiftung.

*Present address: DLR Projekt ARES/ERAS GmbH, Hannah-Vogt-Str.1, D-37085 Göttingen, Germany.
†Present address: Philips RHW, P.O. Box 540240 D-22502 Hamburg, Germany.

[1] W. L. Johnson, Prog. Mater. Sci **30**, 81 (1986).
[2] R. Bormann, Mater. Res. Soc. Symp. Proc. **343**, 169 (1994).
[3] R. W. Bené, J. Appl. Phys. **61**, 1826 (1987).
[4] U. Gösele and K. N. Tu, J. Appl. Phys. **53**, 3252 (1982).
[5] U. Gösele and K. N. Tu, J. Appl. Phys. **66**, 3252 (1989).
[6] E. Ma, C. V. Thompson, and L. A. Clevenger, J. Appl. Phys. **69**, 2211 (1991).
[7] K. R. Coffey, L. A. Clevenger, K. Barmak, D. A. Rudman, and C. V. Thompson, Appl. Phys. Lett. **55**, 853 (1989).
[8] R. W. Balluffi and J. M. Blakely, Thin Solid Films **25**, 363 (1975).
[9] M. Y. Lee and P. A. Bennett, Phys. Rev. Lett. **74**, 4460 (1995).
[10] F. M. dHeurle, P. Gas, and J. Philibert, Mater. Res. Soc. Symp. Proc. **343**, 181 (1994).
[11] F. M. dHeurle, J. de Physique IV (France) **6**, C2-29 (1996).
[12] K. R. Coffey and K. Barmak, Mat. Res. Soc. Symp. Proc. **343**, 193 (1994).
[13] L. G. Harrison, Trans. Faraday Soc. **57**, 1191 (1961).
[14] H. Okamoto and T. B. Massalski, Bull. Alloy Phase Diagrams **4**, 190 (1983).
[15] B. Y. Tsaur and J. W. Mayer, Philos. Mag. A **43**, 345 (1981).
[16] L. Hultman, A. Robertson, H. T. G. Hentzell, I. Engström, and P. A. Psaras, J. Appl. Phys. **62**, 3647 (1987).
[17] F. H. Baumann and W. Schröter, Phys. Rev. B **43**, 6510 (1991).
[18] T. R. Anantharaman and C. Suryanaryana, J. Mater. Sci. **6**, 1111 (1971).
[19] M. von Allmen, S. S. Lau, M. Mäenpää, and B. Y. Tsaur, Appl. Phys. Lett. **36**, 207 (1980).
[20] U. Gnauert *et al.*, (to be published); U. Gnauert, thesis, University of Göttingen, 1994; S. Buschbaum, diploma thesis, University of Göttingen, 1995.
[21] B. Mohadjeri, J. Linnros, B. G. Svensson, and M. Östling, Phys. Rev. Lett. **68**, 1872 (1992).
[22] T. J. Konno and R. Sinclair, Inst. Phys. Conf. Ser. **134**, 173 (1993).
[23] In situ x-ray diffraction data were obtained in the limited 2Θ-range between 40° and 49°. Integrated intensity I_{int} and width w (defined as the FWHM) were obtained by fitting a Gaussian and a constant background to the Au diffraction peaks. Total x-ray diffraction spectra were recorded after *in situ* measurments to confirm silicide formation.
[24] B. D. Cullity, *Elements of X-Ray Diffraction* (Addison-Wesley, Reading, MA, 1978).
[25] DSC experiments obtained at two different heating rates are consistent with two-dimensional growth of the silicide [20], i.e., with an exponent $n = 2$ in the Johnson-Mehl-Avramai kinetics (c.f. [26]). Extrapolation of these data to reaction rates accessible by our *in situ* XRD setup yields reaction temperatures below 90 °C.
[26] J. W. Christian, *Transformations in Metals and Alloys* (Pergamon Press, New York, 1975), Pt. I.
[27] W. H. Wang, H. Y. Bai, Y. Zhang, H. Chen, and W. K. Wang, J. Appl. Phys. **73**, 7217 (1993).
[28] Preparation of cross-section TEM foils using ion-beam thinning at liquid nitrogen temperature resulted in silicide formation even in unreacted samples.
[29] M. Seibt, S. Buschbaum, and U. Gnauert, Inst. Phys. Conf. Ser. **146**, 545 (1995).
[30] S. Coffa, J. M. Poate, D. C. Jacobson, W. Frank, and W. Gustin, Phys. Rev. B **45**, 8355 (1992).
[31] A. A. Pasa, H. R. Paes, and W. Losch, J. Non-Cryst. Solids **137&138**, 1087 (1991).
[32] F. K. LeGoues, V. P. Kesan, S. S. Iyer, J. Tersoff, and R. M. Tromp, Phys. Rev. Lett. **64**, 2038 (1990).
[33] D. E. Jesson, S. J. Pennycook, J.-M. Baribeau, and D. C. Houghton, Phys. Rev. Lett. **68**, 2062 (1992).